Journal of Theoretical and Applied Information Technology
31st May 2023. Vol.101. No 10

ISSN: 1992-8645 www.jatit.org E-ISSN: 1817-3195

ANALYSIS AND CLASSIFICATION OF MALARIA INFECTED ERYTHROCYTES USING MICROSCOPIC IMAGES

SYED AZAR ALI[1] , DR. S. PHANI KUMAR[2]

[1]Research Scholar, CSE Dept., GITAM Deemed to be University, Hyderabad, Telangana, India,

[2]Professor & HOD, CSE Dept, GITAM Deemed to be University, Hyderabad, Telangana, India,

E-mail: [1] syedazarali@gmail.com, [2] phanikumar.s@gmail.com

ABSTRACT

Malaria is a member of a small group of diseases that can be highly severe. The presence of parasites in the environment might lead to sickness in the intestines. To visually identify the parasitemia, is a challenging task. The proposed solution categorizes and analyzes malaria impaired red blood cells. The parasite Plasmodium falciparum is the source of erythrocyte contamination. The system process the data in three phases/stages, the first phase preprocess the data by correcting the difference in luminance, the second phase performs segmentation of image pixels to detect erythrocytes. In the final phase a two stage classification model is used for identification of infected red blood cells. The system utilizes 3000 labeled images as the dataset for the purpose of training and 500 images for testing. The proposed system identifies infectious red blood cells with a Recall of 93% and 98.7% of Specificity. The model could demonstrate a recall of 77.9% and Specificity of 90.9% in identification of the infectious stage.

Keywords: *Malaria Parasites, Feature Extraction, Erythrocytes, AI Characterization, Automatic Analysis*

1. INTRODUCTION

Malaria is a disease that causes a significant number of experiments to be carried out on a regular basis all over the world. Malaria, Vivax malaria, Oval malaria, and Falciparum malaria are the four types of heterogeneous plasmodium parasites that are the primary cause of the disease [1]. Plasmodium falciparum is a deadly strain of the parasite that infects around 3 million to 7 million people on a yearly basis. In order to combat the threat posed by parasites and vectors, a number of effective therapies were devised and put into action over the course of several years. The impact of the disease on the people can be analyzed by performing Sentiment Analysis [2] on Social Media platforms using various methods [3]. To identify the growth of this dangerous parasite various test and approaches are used. These models perform the investigation of development of parasites as well as the effectiveness of therapy in blood strains. Several methods, including osmosis of radio-labeled forerunners, biochemical studies, and fluorometric methodologies, can be utilized to perform a development analysis. Because of their high initial cost and ongoing maintenance requirements, these testing procedures are difficult to implement in developing countries [4]. The skilled and reliable alternative choice is to visually examine any tiny blood strains that may be present. The straining of the plasmodium falciparum parasite makes it possible to categorize erythrocytes and parasites together. Visual examination, on the other hand, is time-consuming and can produce unpredictable results. As a result, computer-assisted parasitemia analysis, using few amounts of blood on films stained with Giemsa, has emerged as a viable solution for treatments for malaria. Examining blood films that have been contaminated with Plasmodium falciparum requires taking into account a number of important factors, including an accurate count of erythrocytes and a prediction of the contamination stage.

These problems are unpleasant as a result of the disparity in the brightness of the photos. This disparity can be explained by a number of factors, including test readiness variations, manufacturing, and the definition of photos taken during. This problem is illustrated in Figure 1

ISSN: 1992-8645 www.jatit.org E-ISSN: 1817-3195

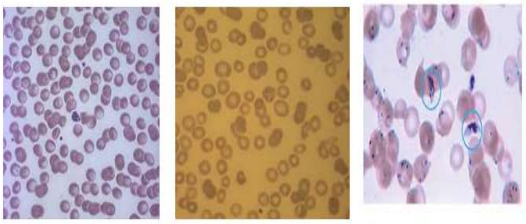

Figure 1: Exceptional shade and brightness characteristics for malaria blood stains

It is possible to see, moving clockwise around the figure from left to right, the various stages that the parasites go through in the above figure, the partly covered cells and in the second the artifacts, and the spotted artifacts and immolated red blood cells in the final. The use of colour approaches suited to climatic conditions ought to be embraced by research centers. These could lead to erroneous investigations and produce a wide variety of multiple occurrences.

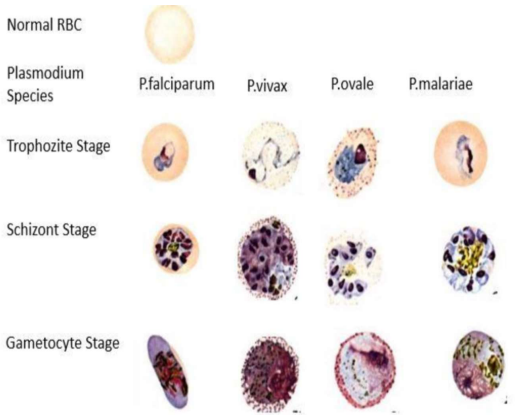

Figure 2: Infected and Healthy Erythrocytes

In order to evaluate antimalarial therapies, it is necessary to determine the life stage of the parasite based on the number of infected erythrocytes. Figure 2 outlines the several stages of Plasmodium falciparum. The various infectious stages are identified through the structural features. In light of the fact that the coverage of highlights is dependent on the layout as well as the experience of the viewer at various phases [5], it is possible that certain patterns would emerge. Erythrocytes have the potential to undergo surface, variety, and shape changes, as seen in the first line in Figure 2. Erythrocytes in the ring stage that have been infected by a parasite are apparent in the second line of Figure2. These erythrocytes may also have many rings. Infected erythrocytes will have trophozoites, which might be difficult to examine due to their location as shown in the next row of the Figure. The last row depicts the schizont stage, which is characterized by the clustering of parasites into an intricate structure inside red cells that contain chromatin specks.

The process of identification of infectious Erythrocytes and their stages can be automated by developing a computerized system utilizing Machine Learning Models.

2. LITERATURE REVIEW

Utilizing computations for heterogeneous picture division allowed for a speedy analysis of regular histology cases. Because the majority of calculations are rarely given to the characterization stage and generally to examination, this unfortunate identification awareness and early recognition of parasite life stage was prompted. Utilizing computations for heterogeneous picture division allowed for a speedy study of routine histology samples. The majority of computations are only rarely committed to the characterization step and generally to the inspection stage, which led to unlucky location aware nesses and the early prediction of the parasite life stage [6]. Cecilia Di Ruberto et al. [7] employed RGB photographs and portioned erythrocytes based on size after acquiring them from a dim scale granulometry examination utilizing watershed calculation. For the arrangement of the schizonts, the Harsdorf distance and morphological tasks were utilized.

In addition to the improvement of early life stage identification through the utilization of neighborhood limits, Ross et al. [8] offered a comparison approach. In this study, a two-stage AI approach was applied in order to separate the different species of parasites by the use of characterization. During the primary stage, the highlights of the picture, such as tone and surface, were used to categorise positive and negative aspects of the picture. The third stage consisted of analysing the infected erythrocytes for characteristics of the parasites such as their size, shape, and variety. In order to evaluate malaria, numerical morphology was applied. The division of erythrocytes using limit work can be achieved by applying edge channel to the shade of the image. Because of the affiliation factor among the edges and the successive employment of parallel morphological activities, it was determined that erythrocyte contamination had occurred.

The discovery of erythrocytes by using a layout matching strategy was proposed by Halim et al. [9]. In this method, individual photos were used to

generate a grayscale format, and then this format was connected with a preset double pattern. Using the quantized picture with eight levels of variation, a three-by-three lattice is constructed. In consideration of the maximum number of co-occurrences, the order of parasites is determined by using pixels. Artificial intelligence is utilized to differentiate between the parasitic sickness. After that, the pixels are categorized as either parasites or non-parasites using a variety of standard numerical morphological administrators, and a k-closest neighbour classifier is used to determine which of the two groups each pixel belongs to.

Maqsood et al. [10] designed a two phase system for efficiently identifying malarial parasites. In the initial phase the authors perform a comparative study of different Deep Learning (DL) systems with their performance evaluation. In the concluding phase a customized CNN system is designed that gives a better performance in comparison with existing DL models. The attributes of RBC are recognized by incorporating techniques such as image augmentation and filtering using bilateral filtering. The image augmentation methods aids in making the CNN system a generalized system that avoids over fitting on the data. The authors utilized the NIH Data of Malaria with the customized CNN model giving an accuracy of 96.82% in identifying malaria from the thin blood smears.

The recent study demonstrates the application of computer vision and ML models in detecting/diagnosing malarial parasites with a better performance. The authors Alharbi et al.[11] presented a collaborative effort, in designing an automated system for diagnosing the presence of malarial parasites in red blood cells. The proposed system utilized XG-Boost, SVM, and neural networks for identifying the presence of malarial parasite in the blood smear. The authors could successfully demonstrate that a CNN model outperforms with an accuracy of 97% than the other ML systems. To improve the performance of classification the authors performed image smoothing prior to classification. The authors used Gabor filtering technique, bilateral filtering for the smoothing process. Further pre-processing was employed and top 80% of features were selected as most informative features for the process of classification.

The authors Ifeanyi [12] et al. developed a mobile app for detecting and diagnosing presence of malarial parasite in blood smear by adopting Structured System Analysis and Design Methodology (SSADM). The model performance is elevated by incorporating a CNN system with end to end feature extraction and categorization. The CNN model is initially trained to give a better performance and then it is deployed in a mobile App. The system functions by capturing the image of blood smear using the camera of the device and then passing the data to the app. The mobile app then classifies the image as infected or non-infected.

The author's Siłka [13] et al. presents a novel CNN model that could successfully diagnose the life threatening disease of malaria with an accuracy of 99.68%. The performance of the proposed CNN model with respect to the various performance evaluators like Precision, Recall and Sensitivity was more superior to the traditional models when done on a large dataset. The authors also performed the analysis of subtypes of malaria with elevated results.

3. PROPOSED METHOD

Figure 3 provides a diagram depicting the overall method of determining the malaria parasitemia. In the pre-handling stage, a neighboring flexible low-pass channel is used for brightness revision in obtained images. The classification of erythrocytes into three distinct stages is the method that is used most frequently. In the beginning, an AI process is employed to characterize the tone of each pixel into a specific variety set. This unique variety set is then used to label each pixel as either the foreground or background. The next step is to group the foreground-marked pixels into the inclusion tree [14]. The clumped shapes are then divided using a method called format matching in the third stage. In order to obtain the ideal erythrocyte, a procedure known as Expectation- maximization is performed, and this is done by comparing it to the clustered shape form. The arrangement of erythrocytes according to 25 elements obtained from previous research is performed using four sets that have been evaluated. The entire process can be broken down into two distinct phases. The first step in the process involves using a binary classifier to determine whether or not an erythrocyte is solid. After that, a multiclass characterization method is applied to the erythrocyte in order to direct to the 3 stages of the life cycle of the contamination, such as the, trophozoite, schizont or ring stage.

3.1 Grouping OF IMAGES

Dataset of Malaria comprised of two categories of images which are infected and uninfected malarial parasites which are compiled on Kaggle [15]. The total image set consists of 27,558 images. used for train, validate and testing to identify the presence of infected malarial parasite.

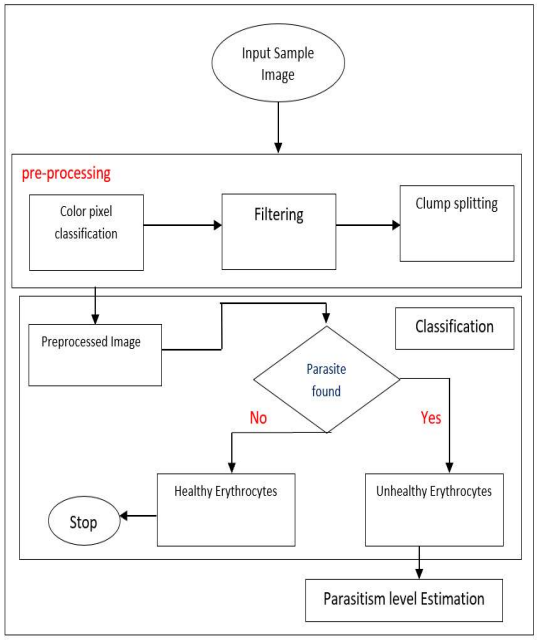

Figure 3: Outline of Proposed Method

4. IMAGE PREPROCESSING

Morphometry is going to be affected by the normalization of infinitesimal techniques. The natural conditions, the film that was used, the thickness of the film, and the colour all play a role in the bending of the picture in ways such as the variety of colors, the brightness, and the size. This leads to complications in the grouping of photos as a result of the ill-advised classification of elements based on their comparative qualities. The use of a nearby low pass channel was necessary in order to reduce the overall brightness of the images. The size of the low-pass channel window was specified such that it could accommodate the substantial picture highlight known as the erythrocyte size. The method of brightness control was applied in order to address the variations that occurred as a result of the varied natural circumstances. In order to separate the luminance and chrominance components of an RGB picture, the YCbCr modification of the ITUR BT.601 standard was applied. The standard deviation of the mean pixel is still unknown after the glorious picture was divided into discrete pieces. For the purpose of storing the low recurrence values, a lattice of a size that is optimized for the disposal of tiling channel influence is utilized. The next step in addressing the brilliance is to get rid of the low frequencies that were obtained. The final image is obtained by making adjustments to brightness and chrominance data, and then using those changes. The results of the pre-handling phase are presented in Figure 4. The picture on the left has not been changed, but the one on the right has been altered.

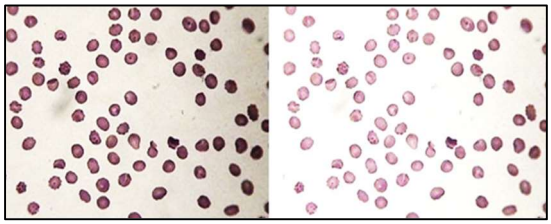

Figure 4: Pre-processed Image

4.1 ID OF ERYTHROCYTES

It is possible to identify erythrocytes based on the result picture of the pre-handling stage. Every image pixel is laid out and labelled in accordance with the tone that serves as the frontal region or foundation. A consideration tree structure is designed to handle frontal area and foundation varied levels connection in order to remove the relics that are produced as a result of staining or digitization. This is done so that the relics can be eliminated.

4.1.1 Classification of Colors

The arrangement of the variety set helps with separating the objects that are in the foreground from those that are in the foundation. The many variety sets are utilized in the construction of a pixel characterization model, which is then used to emphasize key features when looking through things. Calculations based on artificial intelligence, such as Gullible Bayes, SVM, and K-NN, are used for characterization since these methods produce the best results.

4.1.2 Labelling image pixels

The described variety set is used as a query table in order to assign markings as foundation or foreground to every pixel in the image. Figure 5 provides a schematic representation of this cycle.

Journal of Theoretical and Applied Information Technology
31st May 2023. Vol.101. No 10

ISSN: 1992-8645 www.jatit.org E-ISSN: 1817-3195

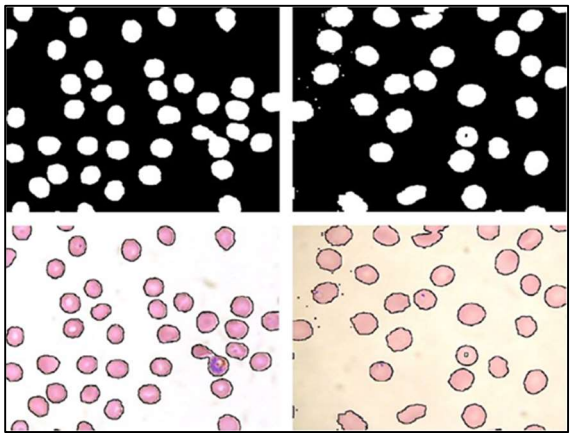

Figure 5: Pixel named picture is show in top two areas and superimposition on portioned erythrocytes is displayed in base segment

5. TRANSLATION OF INCLUSION TREE

The method on inclusion tree is taken into consideration as suggested by authors of [16]. The parallel picture that was obtained has a great deal of information that may be classified according to segments, relationships, and characteristics [17]. Sifting procedures are performed in order to eliminate the level zones in a way that does not impact the boundaries of the remaining segments. In order to construct a zonal chart, associated parts are used, the curves of which address contiguousness, and the vertices of which are segments of P(x). When the process of determining availability using proximity is complete, vertices in a Zonal Graph can be merged or recolored. The consolidated and recolored associated administrators are located in the hubs of the tree [18], which are in view of the progressive connections.

The following steps are taken in order to develop the consideration tree for the proposed work: After the first two associated part trees, consisting of lower (0) and higher (255), have been constructed, the erythrocyte holes in each lower tree's worth of linked part have been examined. These apertures can be found among the tree's upper esteem. The kids and opening that can be found in the upper tree are given as allotment for the corresponding spring portion in the lower tree esteem. The lower tree value and the similar spring in the upper tree value are then joined at that point [14] .In the subsequent consideration tree, there are just the things that are in the foundation and the forefront. Erythrocytes can then be recognized by removing unnecessary data during the process of applying linked administrators. Erythrocytes that are covering picture limits are removed since they are insufficient.

5.1 Isolating Erythrocytes Clumped

In the process of evaluating stained cells, the number of linked cells is an important factor to take into account. This work proposes a novel method based approach for isolating erythrocytes bunched. The method matches the layout of the previous work. The technique was conceived with the goal of locating a similarity between the ideal arrangement and erythrocyte clustered and employing that similarity in the division process. Incorporating an Expectation-expansion Algorithm into the Development of a Template Regarding the evolution of the cell architecture, we anticipate that every single cell that is taken from the picture represents one instance of an actual model. It is believed that each one is the result of a cycle that modifies the actual model by introducing an irregular noise. This noise models the complex interaction of various factors, such as the natural variability, the histology approach, and the enlightenment catching settings.

"Let $D_i = (D^1_i ; ...; D^n_i)$ be a vector of n components, which stores the n parallel pixel upsides of a solitary cell picture, with I = 1...N and N the quantity of single cells extracted from the picture." Allow I to be a vector of n components as well, which represents the pixel upsides of the best cell (genuine model) so that

$$D^i_j = T_i\ (I^j) \tag{1}$$

where T is a stochastic capacity that creates the model occurrence and is characterized as follows

$$T_i\ (1) = \begin{cases} 1\ with\ probability\ pi \\ 0\ with\ probability\ 1 - pi \end{cases} \tag{2}$$

$$T_i\ (0) = \begin{cases} 1\ with\ probability\ 1 - qi \\ 0\ with\ probability\ qi \end{cases} \tag{3}$$

$$(p,q,I) = \underset{p,q,I}{\operatorname{argmax}}\ (L(D \mid p, q, I)) \tag{4}$$

where the likelihood

$$L(D|p,q,I) = \prod_{i=1}^{N} \prod_{i=1}^{n} p(Di\ j|pi,qi,Ij\ ) = \prod_{i=1}^{N} \prod_{i=1}^{n} p(Di\ j|pi,qi,Ij = 1)Ij\ p(Di\ j\ |pi,qi,Ij = 0)1\text{-}Ij \tag{5}$$

$$= \prod_{i=1}^{N} \prod_{i=1}^{n} p^{Ij\ D_i j}\, q^{(1-Ij)(1-Dj)} (1-p_i)^{Ij(1-D_i j)} (1-q_i)^{(1-Ij)D_i j}$$

Where p_i and q_i control the likelihood of mistake on the created occurrence. A T_i with $p_i = q_i = 1$ implies that examples produced by T_i corresponds to the genuine model. The issue is then to find the p_i and q_i values which expand the probability of the examples being produced from the model. The starting boundary gauges p_i and q_i are set to 0.9, as the central speculation in this work is that the occurrences don't contrast a lot from the genuine model. The last assessment of I compares to the genuine model that will be subsequently utilized as a layout to track down cells in the information picture.

5.1.1 Isolating through format matching methodology

The proposed method makes use of a fundamental form of both the layout and the grouped shape by means of a chain code portrayal. This portrayal searches for a dock point that results in a "best match" when the two forms are superimposed on one another. The item limit is typically addressed with the use of a chain code, which is essentially a grouping of straight-line segments along with their respective headers. As the item limit's underlying point, a pixel is selected at random from the pool of available options. After some time has passed, the neighbours of the pixel are given numbers ranging from 0 to 7 (8-neighbor cover), and the pixels that have a position with the limit are selected while moving in a clockwise direction. The got chain code has, at long last, been standardized in order to accomplish an invariant portrayal with regard to the underlying point and direction [19].

6. ERYTHROCYTES CLASSIFICATION

The organization of erythrocytes requires more complicated examples, which should include shape, surface, force, and diversity. A complicated mixture provides a deeper understanding of the contaminated erythrocytes. These important level nuances need to be identified by the smart order in a picture.

6.1 Feature Extraction

The method of highlight extraction separates the significant aspects of a picture so that it can be used to differentiate between healthy and diseased erythrocytes and stages of the disease. Variations in the cytoplasm and chromatin patches of Plasmodium falciparum make it possible to characterize and identify the parasite. The alterations have the same effect as shifts in the circulation of highlights during the extraction process. We model the image as an irregular variable, and its representation is provided by the work associated with its relating likelihood thickness. The components of an erythrocyte are depicted using a number of histograms.

- Tamura surface histogram
- Dim scale
- Sobel histogram
- Variety histogram
- Immersion level histogram

As fundamental descriptors of the histogram attributes, the mean, standard deviation, skewness, kurtosis, and entropy are utilized. In a nutshell, a picture is characterized by 25 highlights that show 5 histograms, with each histogram being addressed by 5 highlights specific to that histogram.

6.2 Classification

Parasite order is done in two stages. The classifier determines whether or not erythrocytes are contaminated during the first stage of the process, and then four different learning models are used to determine the type of disease. An examination is carried out to identify the antiquity class of solid erythrocytes that have been incorrectly identified as polluted. The client is given the opportunity to make a visual selection from among the remaining erythrocytes. This is the motivation behind the utilization of the nonlinear SVM [20] and MLP [21] classifiers.

6.3 Assessment of Model

Classifiers are created on their own using the learning bounds as a guide. For the purpose of SVM preparation, polynomial and radial premise capacities are investigated. In the Radial premise work, the c boundary was moved from 0.1 to 2 with an increment step of 0.1, and the polynomial degree was placed at 1, 2, and 3. After that, the regularisation boundary C was adjusted somewhere between the numbers 1 and 20, with increments of 0.2 in each direction. The performance of the MLP was optimised by varying the number of neurons present in the hidden layer between the values of 1 and 9, and by adjusting the value of the learning rate between the values of 0.1 and 2.0, with a starting point of 0.1.

The F-measure is a useful tool for assessing both

performance and accuracy, and it is defined as follows:

$$F_{\beta} = \frac{TPr * Pr}{\beta * Tpr + (1-\beta) * pr} \quad (6)$$

With

$$TPR = \frac{TP}{Tp+FN} \; PR = \frac{TP}{Tp+FN} \quad (7)$$

where TP stands for the genuine positives, FN for the fictitious negatives, and FP for the deceptive positives. The b coefficient, which ranges from 0 to 1 and has a minimum value of b, makes it possible to reduce relative loads to both the real positive and accuracy rates [22]. In the course of this research, the value of Fb was calculated by setting b to 0.4; hence, the search focused on locating TP.

7. EXPERIMENTAL RESULTS

The performance evaluation of the proposed solution is carried out in 2 stages: Infectious erythrocyte identification and Parasitemia stage identification. Calculation of parasitemia, which comprised digitization of five specific fragile blood films, are both used to evaluate the presentation of the proposed method. Both of these stages are used in the evaluation process. In total, 500 digital photos were utilized for the evaluation process.

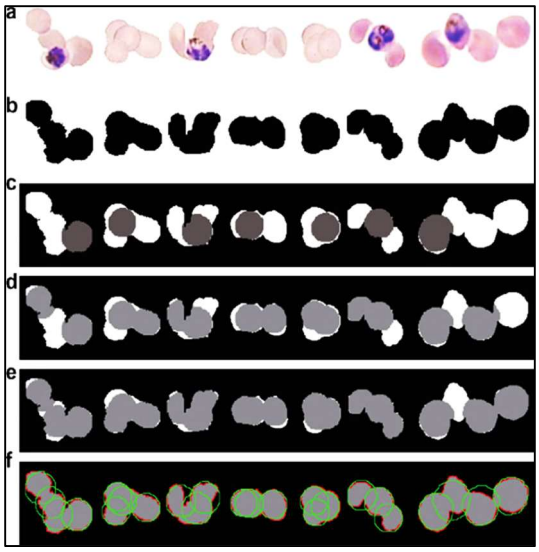

Figure 7: The process of segmentation. The colour red is used to address the accumulated shape. The shape of the found cells is represented in green.

The performance of the proposed clump segmentation algorithm is evaluated here. Figure 7 presents an illustration of the segmentation process. The clumped erythrocytes can be identified in Row 'a', which exhibits a degree of overlapping that contributes to the clumped shape seen in Row 'b' as a result of variations in brightness and hue. Row 'b' displays the binary images that were produced when the segmentation process was completed. The process of segmentation is illustrated in Row 'c', which refers to the first-best matching, Row 'd', which refers to the second-best matching, and Row 'e', which refers to the third-best matching in a sequential order. The findings obtained are unaffected by the amount of overlap that was present. This is a robust method. Row 'f' provides a visual representation of the original clumped contour, which has been superimposed with discrete regions at which the template has acquired a relevant shape. The findings demonstrate that the method that was proposed is able to ascertain the irregular degree of overlapping.

A semi-automatic method was used to examine one hundred randomly selected digital photographs for the presence of erythrocytes. Either manually or by utilising a semi-automatic method, the erythrocytes that are located at the limits of the sample were not taken into consideration. A comparison of manual and semi-automatic methods for estimating erythrocyte counts was used to evaluate the performance of the method. In the second column of Table 1, the arithmetic mean and cumulative average are displayed for both Expert 1 and Expert 2. In column three, the percentage of incorrectly counted cells in terms of the total number of cells is expressed. The proposed method has an average error of 0.16% and a standard deviation of 5.59, which is quite close to the arithmetic mean of the experts. The results of the correlation showed that there was a high connection between experts and the semi-automatic technique, as shown in Table 2.

Table 1: Evaluation of erythrocytes using the suggested approach and ocular evaluation

	Avg difference	% Difference
Expert 1	0.23	1.23 ± 6.42
Expert 2	0.26	1.66 ± 5.56
Expert mean	0.04	0.16 ± 6.39

Table 2: Association between expert evaluation and semi-automatic approach

	Expert 1	Expert 2	Automatic
Expert 1	1.000		
Expert 2	0.993	1.000	
Automatic	0.992	0.977	1.000

A significant difference was brought about by the covering cells that were not divided, as well as by the cells at the edges that were included by specialists.

7.1 Parasitemia Assessment

The evaluation of the parasitemia and life stage examination was done by using the complete dataset, partitioned it into 40% for training, 30% for validation, and 30% for testing. The validation and training set was used for fine tuning of classification system's border. In order to evaluate the performance, the test set was utilized. By naturally differentiating the erythrocytes, which were then altered using the ID procedure that was discussed in the previous part, new image documents were created and saved. These are referred to by specialists as the sound, the trophozoite, the ring, or the schizont. A total of 13,446 erythrocytes, including 10,955 healthy erythrocytes, 490 infected with the disease in its ring stage, 110 infected with the disease in its trophozoite stage, and 94 infected with the disease in its schizont stage, were used.

Identifying erythrocytes that were contaminated.

In the first stage of the grouping process, the erythrocytes were laid out in their complete configuration. The Fb measure is used to evaluate a person's level of proficiency. Figure 8 presents the shape plots of the F_b measure for both the MLP and the SVM. The dark regions represent the best performance parameters. Each worth of F_b is produced using a tenfold cross-approval method that makes use of 10 trials. It was consistently possible to get a productivity of 0.91 in the results. A superior execution was achieved with values between 1.3 and 1.9 and with small difficulty values. Therefore, the ideal blend of the boundary conditions c and C was set at 1.3 and 3, which resulted in a normal Fb value of 0.941. Better execution was accounted for by degree 2 and varied difficulties when using the SVM with the polynomial section. By doing things this way, the level of difficulty was set at 3, which resulted in a Fb proportion of 0.948. After much deliberation, the optimal parameters for the MLP were determined to be 8 neurons in the secret layer, a learning pace of 0.2, and a Fb value of 0.925.

Table 3 provides an outline of the completed order of approval and test sets, which was accomplished through the utilization of enhanced learning models. Every single learning model is successful in reaching a viability of 0.93. The number of false negatives was exceptionally low, and the majority of patients had early stages of the disease. The process of staining relics did not result in very many false positives either.

The SVM classifier was able to achieve superior performance, as shown in table 3, despite having a polynomial component with a degree of 2 and a complexity of 3. When it came to the identification of tainted erythrocytes. SVM was able to achieve a responsiveness of 95% and an explicitness of 99.6% in the whole informative collection.

Table 3: F_b optimum measurements for the SVM with a polynomial piece, the SVM with a spiral section, and the MLP, as well as approval and test sets for the tainted erythrocyte recognition procedure

	SVM_RBF =.8, C=4	SVM Poly P=2,C=3	MLP neurons=7, I_rate=0.1
Training Set	0.95	0.947	0.935
Validation Set	0.946	0.966	0.945
Test Set	0.944	0.971	0.946

7.2 Contamination Stage Identification

In a previous stage, 700 erythrocytes were identified as polluted; currently, these are being examined for the purpose of recognizing the illness stage. Every classifier makes use of the best boundaries that were chosen by employing the cycle that was described in the previous sections. As a consequence of this, 654 erythrocytes were organized, and 46 of them were ambiguous or might be placed in more than one category.

Table 4: In The Automatic Infection Stage Categorization Process, F_b Measurements For Training, Validation, And Test Sets

	Ring Stage	Schizont	Throphozoite
	MLP neurons=7 I_rate =0.1	SVM _RBF C=0.2 C=14	SVM _RBF C=0.2 C=12.4
Training Set	0.947	0.781	0.79
Validation Set	0.955	0.528	0.742
Test Set	0.961	0.772	0.892

Table 4 includes the Fb measure that was naturally obtained from planned occurrences for the purpose of approval and setting up a preparation set. This table also displays the best classifier for each type of contamination. In comparison to the other classes, the execution in ring stage was superior. This result is attributable to the fact that this class had a greater number of exams than the others. As a result, a model with a more precise order can be worked out for this class.

A MLP classifier with 7 neurons in the secret layer and a learning pace of 0.1 was used to naturally group the erythrocytes that were contaminated at this stage, achieving a viability of 95%, a responsiveness of 99.1%, and an explicitness of 80.4% in the process. The total number of erythrocytes that were contaminated was 464. It is possible that the lacklustre performance of the Trophozoite class is attributable to the fact that this class is associated with the transitional phase of the parasite from the ring to the schizont stage. For instance, erythrocytes of other disease classes have similar qualities like erythrocytes of this class.

7.3 User Assessment for classification

When the arrangement of classifiers fails to assign erythrocytes to a specific category, it is essential for the customer to provide their own visual characterization of the samples. Only 54 assessed erythrocytes were left for client arrangement after a total of 12600 were examined; this represents 0.4% of all cells. In total, there were 16 solid erythrocytes, 20 ring contamination, and 10 trophozoite contamination. Because of the assistance of customers, the process of identifying erythrocytes that were contaminated with ring and trophozoite expanded.

Table 5: F_b Measures Of Training, Validation And Test Sets After User Assistance.

	Infected Erythrocytes	Ring Stage	Schizont	Throphozoite
Training Set	0.962	0.947	0.78	0
Validation Set	0.972	0.966	0.732	0
Test Set	0.981	0.971	0.882	0

When the arrangement of classifiers fails to assign erythrocytes to a specific category, it is essential for the customer to provide their own visual characterization of the samples. Only 54 assessed erythrocytes were left for client arrangement after a total of 12600 were examined; this represents 0.4% of all cells. In total, there were 16 solid erythrocytes, 20 ring contamination, and 10 trophozoite contamination. Because of the assistance of customers, the process of identifying erythrocytes that were contaminated with ring and trophozoite expanded. After receiving assistance from the customer with grouping, the final proficiency of the framework is presented in Table 5. The efficiency and explicitness of identifying polluted erythrocytes increased to 97.2% and 99.9% respectively. During the trophozoite stage, responsiveness increased from 62.4% to 66.7%, while effectiveness increased from 67.1% to 71.1%. During the ring stage, however, proficiency and awareness increased to 94.9 and 99.2 respectively.

8. CONCLUSION

The review that has been offered provides an innovative approach to dealing with the order and investigation of contaminated erythrocytes at their level of contamination. The separation of each category is accomplished by employing a variety of classifiers that make use of low-level elements that are extracted in a natural manner from digital photographs. We tested a total of 500 images, each of which comprised 12600 erythrocytes and had a parasitemia level of 6.1%. We were successful in achieving 99.8% specificity and 95% responsiveness. The photographs that were randomly selected from the delicate blood film

displayed a diverse range of variety, brilliance variations, and heterogeneous thickness. At neither the microscopical procurement settings nor the histological methods, any standard tactics were utilized. The photographs that were obtained through digitalization were very bright and displayed complexities in staining separation and relics, both of which were difficult to judge even by the visual characterization of the customer. For the purpose of enhancing the foundation magnificence of these antiques while simultaneously protecting the closer view things, neighborhood low pass sifting was applied. As a result, the implementation of the pixel classifier was improved in order to achieve foundational perfection. The proposed framework investigated the erythrocyte-parasite relationship as a whole and used this information to determine whether or not an erythrocyte is contaminated in conjunction with its disease stage. As demonstrated by the findings, the proposed method is successful in producing evidence that can be used to verify the presence of contaminated erythrocytes. The suggested method performs binarization on images by making use of the master data and a prepared classifier that assigns each pixel to a certain category within an RGB-standardized space. A client addition that is relatively unimportant is anticipated to select test pixels for the purpose of producing factual classifiers. After that, objects are constructed out of individual pixels using consideration trees. Cells that overlap one another prevent the erythrocyte order from being completely digitized and computerized. This method is capable of separating 95% of the grouped forms in the test images. The framework arrives at a conclusion regarding the amount of faith in the scheduled results and grants the client the ability to arrange for a low certainty level outside. Based on the findings presented above, it was discovered that just 0.4% of the items needed to be evaluated by the master client. This method is successfully versatile for the separation of various living beings in microscopical pictures due to the utilization of nonexclusive example acknowledgment calculations. The work can be extended by considering various textual features and statistical features which can further be used to analyze the species of malarial parasite. The method can be improved using CNN [23]

REFERENCES

[1] Syed Azar Ali, Dr. S. PhaniKumar, "Review of Decision Tree based binary Classification using Robust 3D and Feature Selection for Malaria Infected Erythrocyte Detection", Data Engineering and Communication Technology Proceedings of 3rd ICDECT-2K19, Editors: K. Srujan Raju Roman Senkerik Satya Prasad Lanka V. Rajagopal, Book Chapter, ISBN 978-981-15-1096-0

[2] S. Fouzia Sayeedunnisa, N.P. Hegde & K.U.R. Khan," Wilcoxon Signed Rank Based Feature Selection for Sentiment Classification". In Proceedings of the Second In- ternational Conference on Computational Intelligence and Informatics, 2018. pp. 293-310.

[3] S.Fouzia Sayeedunnisa, N.P. Hegde & K.U.R. Khan, "Feature Selection by Associativity for Sentiment Analysis". In Smart Computing Techniques and Applications, 2021. pp. 423-430

[4] Md. Jaffar Sadiq, Dr. V.V.S.S.S. Balaram, "Review of Microscopic Image Processing techniques towards Malaria Infected Erythrocyte Detection from Thin Blood Smears" International Journal of Scientific & Engineering Research Volume 8, Issue 6, June-2017

[5] MD. Riyazuddin, Dr. V.V.S.S.S. Balaram, "Diversity Scale by Supervised Learning for Privacy Preserved and Informative Data Publishing" Parishodh Journal Volume IX, Issue II, February/2020, ISSN NO:2347-6648, Page No:872

[6] MD. Riyazuddin, Dr. V.V.S.S.S. Balaram, "Pattern Anonymization: Hybridizing Data Restructure with Feature Set Partitioning for Privacy Preserving in Supervised Learning" SpringerScience+Business Media Singapore 2017, AISC series, S.C. Satapathy et al. (eds.), Proceedings of the First International Conference on Computational Intelligence and Informatics, Advances in Intelligent Systems and Computing 507, DOI 10.1007/978-981-10-2471-9_58, Page No. 594 – 604

[7] Ruberto CD, Dempster A, Khan S, Jarra B. Analysis of infected blood cell images using morphological operators. Image Vision Comput2002; 20:133–46.

[8] Ross NE, Pritchard CJ, Rubin DM, Dusé AG. Automated image processing method for the diagnosis and classification of malaria on thin blood smears. Med Biol EngComput2006; 44:427–36.

[9] Halim S, Bretschneider TR, Li Y, Preiser PR, Kuss C. Estimating malaria parasitaemia from blood smear images. In: Proceedings of the IEEE international conference on control, automation, robotics and vision; 2006

[10] Maqsood A, Farid MS, Khan MH, Grzegorzek M. Deep malaria parasite detection in thin blood smear microscopic images. Applied Sciences. 2021 Mar 4;Volume11(5) Page No:2284.

[11] Alharbi AH, Lin M, Ashwini B, Jabarulla MY, Shah MA. Detection of peripheral malarial parasites in blood smears using deep learning models. Computational Intelligence and Neuroscience. 2022 May 24;2022. https://doi.org/10.1155/2022/3922763.

[12] Ifeanyi OC, Ajayi BA, Abdullahi MU. Malaria disease detection system based on convolutional neural network (CNN).2022. https://doi.org/10.30574/wjarr.2022.16.3.1304.

[13] Siłka W, Wieczorek M, Siłka J, Woźniak M. Malaria Detection Using Advanced Deep Learning Architecture. Sensors. 2023 Jan;2023(3) Pages:1501.

[14] Monasse P, Guichard F. Fast computation of a contrast-invariant image representation. IEEE Trans Image Process 2000; 9:860–72.

[15]https://www.kaggle.com/code/nithincleetus/malaria-cell-detection/input

[16] Díaz G, González FA, Romero E. A semi-automatic method for quantification and classification of erythrocytes infected with malaria parasites in microscopic images. Journal of biomedical informatics. 2009 Apr 1;Volume 42(2) Pages:296-307

[17] Heijmans HJAM. Connected morphological operators for binary images.Comput Vis Image Understand: CVIU 1999;73(1):99–120.

[18] Braga-Neto U. Multiscale connected operators. J Math Imag Vis2005; 22:199–216.

[19] Dempster A, Laird N, Rubin D. Maximum likelihood from incomplete data via the EM algorithm. J R Stat Soc 1977; 39:1–38.

[20] Vapnik VN. The nature of statistical learning theory. Springer-Verlag; 1989.

[21] Carling A. Introducing neural networks. Sigma Press; 1992.

[22] Daskalaki S, Kopanas I, Avouris N. Evaluation of classifiers for an uneven class distribution problem. Appl ArtifIntell2006; 20:381–417.

[23] Bairagi VK, Charpe KC. Comparison of texture features used for classification of life stages of malaria parasite. International Journal of Biomedical Imaging. 2016 Apr;2016.